J Mater Sci (2007) 42:9966–9972
DOI 10.1007/s10853-007-2074-z

An investigation on synthesis and photocatalytic activity of polyaniline sensitized nanocrystalline TiO_2 composites

Shixiong Min · Fang Wang · Yuqi Han

Received: 2 April 2007 / Accepted: 30 July 2007 / Published online: 22 September 2007

Abstract Polyaniline (PAn) sensitized nanocrystalline TiO_2 composite photocatalyst (PAn/TiO_2) with high activity and easy separation was facilely prepared by in situ chemical oxidation of aniline from the surfaces of the TiO_2 nanoparticles. The morphology, structure, and light absorption properties of composite photocatalyst were examined in term of its application to photocatalysis. The photocatalytic activity of PAn/TiO_2 nanocomposites for the degradation of methylene blue (MB) aqueous solution was investigated and compared with pure TiO_2. The spectra analyses illustrated that, when PAn deposited on the surface of TiO_2, the crystalline behavior of PAn was hampered and the degree of crystallinity decreased, and the characteristic peaks of the PAn were shifted indicating that there was a strong interaction between PAn and TiO_2 nanoparticles. PAn was able to sensitize TiO_2 efficiently and the composite photocatalyst could be activated by absorbing both the ultraviolet and visible light (λ = 190–800 nm), whereas pure TiO_2 absorbed ultraviolet light only ($\lambda < 400$ nm). Photocatalytic experiments showed that under natural light irradiation, MB could be degraded more efficiently on the PAn/TiO_2 than on the pure TiO_2, due to the charge transfer from PAn to TiO_2 and efficient separation of e^--h^+ pairs on the interface of PAn and TiO_2 in the excited state. More significantly, the PAn/TiO_2 composite photocatalyst exhibited easy separation and less deactivation after several runs. The advantages of the obtained PAn/TiO_2 composite photocatalyst revealed its great practical potential in wastewater treatment.

S. Min (✉) · F. Wang · Y. Han
Department of Chemistry, Key Laboratory of Resources and Environmental Chemistry of West China, Hexi University, Zhangye, Gansu 734000, China
e-mail: msxwf@yahoo.com.cn

Introduction

Semiconductor titanium dioxide in the anatase form is a promising material for photoelectric conversion and photocatalytic treatment of pollutants from water and air because it has the reasonable photoactivity under ultraviolet light irradiation ($\lambda < 380$ nm) and the advantages of being not toxic, insoluble, and comparatively inexpensive [1]. The photocatalytic properties of titanium dioxide particles have been investigated extensively in slurry cell and as immobilized films [2–5]. However, the low solar energy conversion efficiency and the high charge recombination rate of photogenerated electrons and holes are often two major limiting factors for its widely practical applications [5]. In order to utilize the main part of the solar spectrum and even poor irradiation of interior lighting more effectively in the photocatalytic reactions, the TiO_2-based photocatalyst that can yield highly reactivity under visible light irradiation should be developed. For this purpose, several attempts have been made to increase the photocatalytic efficiency of TiO_2, such as dye photosensitization [6, 7], ion doping [8, 9], and forming its reduced form such as n-$TiO_{2-x}N_x$ [10]. However, most of these catalysts suffer from a stability problem such as dissolution and the photocatalytic degradation of the dyes, an increase of carrier-recombination centers, or the requirement of an expensive facility and relatively long reaction time. In addition, several drawbacks such as deactivation and separation of fine catalyst powders from the aqueous phase after use, prevents the large-scale applications of this promising method. From a practical point of view, other processes for endowing TiO_2 with a visible light response, good sedimentation ability, and less deactivation are still desirable.

Conjugated polymers (CP's) with extend π-conjugated electron systems such as polyaniline, polythiophene,

polypyrrole, and their derivatives, etc have shown great promises due to their high absorption coefficients in the visible part of the spectrum, high mobility of charge carriers, and good stability [11]. Furthermore, many CPs in their doped or undoped states are efficient electron donor and good holes transporter upon visible light excitation [12]. Therefore, recently, conjugated polymers act as stable photo-sensitizer combined with wide band gap inorganic semiconductors (e.g., TiO_2, CdS, and CdSe) was an emerging area of research for optical, electronic, and photoelectric conversion applications. And various composites with different combinations of the two components composition have been reported in the literature [13–22]. While in these composites, the relatively high photoelectric conversion efficiency can be realized and charge transfer from conjugated polymer to semiconductor has been extensively demonstrated, very little work have been done to directly study the photocatalytic activity of these materials under visible light irradiation.

In the present work, a facile in situ polymerization method was employed, aiming to develop a new form of nanometer polyaniline sensitized TiO_2 composite photocatalyst with the following advantages: (i) It exhibits high photocatalytic activity and low deactivation under natural light irradiation. (ii) The photocatalyst can be separated from the aqueous phase after use by simple gravity settling. The prepared composite photocatalyst was characterized by TEM, XRD, FT-IR, UV–vis, and ESR techniques. Under the natural light irradiation and in the presence of oxygen only from air, the photocatalytic activity of the polyaniline/TiO_2 composite photocatalyst was investigated for the photodegradation of methylene blue (MB) in a suspension system to evaluate the potential application of this kind material in the disposal of pollutants.

Experimental

Materials and regents

Aniline (ANI) monomer (AR, Beijing Chemical Reagent Co., China) was distilled two times under reduced pressure and stored below 4 °C under nitrogen atmosphere. Nanocrystalline TiO_2 (Anatase, average size of 80 nm, Beijing Chemical Industrial Co., Ltd., China) and all other reagents, including ammonia persulfate ($(NH_4)_2S_2O_8$, APS) and concentrated hydrochloric (HCl), were of analytical grade regents and used as received. Water used in this work was deionized water.

Preparation of PAn/TiO_2 nanocomposites

PAn/TiO_2 nanocomposites were facilely prepared by the in situ chemical oxidative polymerization of aniline on the surface of TiO_2 with a dispersion polymerization method. The typical process was carried out as follows: about 1.0 g TiO_2 was dispersed into 250 mL 1.2 M HCl aqueous solution containing 0.30 mL aniline with ultrasonic vibrations for 2 h. This procedure was necessary for both reducing the agglomeration of TiO_2 nanoparticles and absorbing aniline on its surface. The 0.735 g $(NH_4)_2S_2O_8$ was dissolved in 10 mL of 1.2 M HCl and drop-added into the dispersoid within 20 min under stirring. The polymerization was allowed to proceed for 12 h at room temperature (30 °C). Afterward, reaction mixture was filtered under gravity and washed with 1.2 M HCl and large amount of deionized water each for three times in turn. The resulting products, polyaniline/TiO_2 (PAn/TiO_2) were dried at 60 °C for 24 h under vacuum to obtain fine white green powders.

Instruments and analytical methods

The morphology of the PAn/TiO_2 nanocomposites was observed on a JEM-1200EX/S transmission electron microscope (TEM); the powders were dispersed in anhydrous ethanol in an ultrasonic bath for 5 min, and then deposited on a copper grid covered with a perforated carbon film. The crystalline structure of the nanocomposites was taken on a Rigaku D/MAX-2400 X-ray diffraction spectrometer with a Cu Kα X-ray radiation (λ = 0.154 nm). IR spectra were characterized with DIGILAB FTS-3000 FT-IR spectrometer; the samples were palletized with KBr. The diffuse reflectance spectra were recorded by Shimadzu UV-2550 ultraviolet spectrometer using an integrating sphere and $BaSO_4$ as a white standard. ESR spectra was recorded on Bruker ER 200D-SRC electron paramagnetic resonator with modulated frequency of 100 kHz, microwave frequency of 9.58 GHz, time constant of 1 s, and intensity of magnetic field from 400 to 3,456 G.

Photocatalytic experiments

The photocatalytic activity of nanometer PAn/TiO_2 nanocomposites was estimated by measuring the decolorization rates of MB. The photocatalytic experiments were conducted in October 2006, over a continuous 5 day period. All experiments were done inside the room of chemistry department building in an open atmosphere between 11.00 a.m. and 1.00 p.m. The sky is clear and the sunrays are very intense in this period in the city of Zhangye (latitude: 38°56′11″N; longitude: 100°27′21″E), Gansu (China). Natural light illumination was performed in a 100 mL beaker at room temperature (30 °C). In all experiments, 50 mL of MB (10 mg/L, pH 6.8) and 100 mg

of catalysts was suspended and immediately stirred during illumination. At given intervals of illumination, a sample of the catalysts particulate was collected, centrifuged. The supernatant were analyzed by Unico 2100 spectrophotometer at λ_{max} = 665 nm. The determined absorption was converted to concentration through the standard curve method of dyes (r = 0.99884). By this method conversion percent of MB could be obtained in different intervals. The photocatalytic decolorization efficiency (D_t%) was given by following equation:

$$D_t\% = \frac{C_0 - C_t}{C_0} \times 100\%$$

where C_0 was initial concentration of MB and C_t for concentration at time t.

The catalysts were used repeatedly; 100 mg catalyst powder was added into 50 mL of 10 mg/L MB solution, magnetically stirred under natural light irradiation for 90 min. After centrifuging, the supernatant solution was discarded and replaced with 50 mL fresh MB solution, and the remaining catalyst was reused for the next run.

Sedimentation ability tests

The sedimentation ability of catalysts was evaluated as follows: 50 mL of an aqueous solution of the catalyst at a concentration of 2 g/L was placed in a 100 mL graduated cylinder and was stirred vigorously for 30 min. Then the solid catalyst was allowed to settle under gravity. The height of the solid–liquid interface was then measured using the graduations on the cylinder at various time intervals.

Results and discussion

Size, morphology and crystalline structure

The TEM photographs of TiO_2 nanoparticles and PAn/TiO_2 nanocomposites are shown in Fig. 1. As shown in Fig. 1a, the original commercially available nanocrystalline TiO_2 particles are aggregated in anhydrous ethanol with an irregular shape and the size is in the range of 80–120 nm, centered at about 100 nm. This should be attributed to the high surface energy of nanoparticles. From Fig. 1b, it can be seen that the morphology of composite particles does not differ much from that of TiO_2 nanoparticles and the average particles size is close to that of the TiO_2 nanoparticles. However, some of particles in the composites tend to form multiparticles aggregation and heap tightly than pure TiO_2. It can be thought that there are two kinds of particles in the composites. One is free PAn particles, and the other is the PAn-coated TiO_2 composite particles. The composite particles are may be glued or bound by the PAn chains acting as binders in the nanocomposites. Due to the extreme thinness of the PAn shell, it is impossible to make it visible in the TEM photographs. It has been reported that when the thickness of the polymers is down to the exciton diffusion length ($\approx$20 nm) and the CP's and TiO_2 is closely linked together, the photo-induced charge transfer from the CP's to TiO_2 is possible and much quicker, and hence an efficient charge separation should be realized [23]. Moreover, PAn/TiO_2 composite particles with small size can exhibit much larger efficient areas and more efficient active center, which is in favor of the preadsorption of organic pollutants and following degradation when it is used as catalyst.

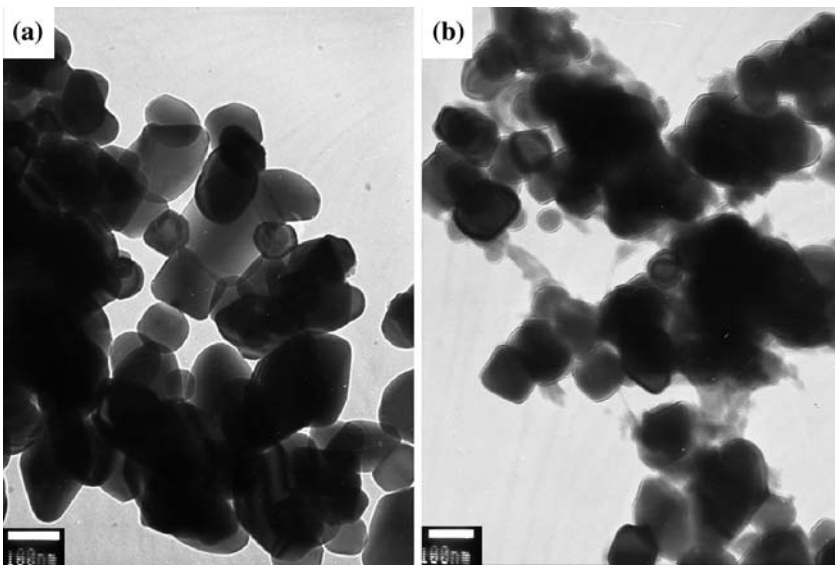

Fig. 1 The TEM photographs of TiO_2 nanoparticles (**a**) and PAn/TiO_2 nanocomposites (**b**)

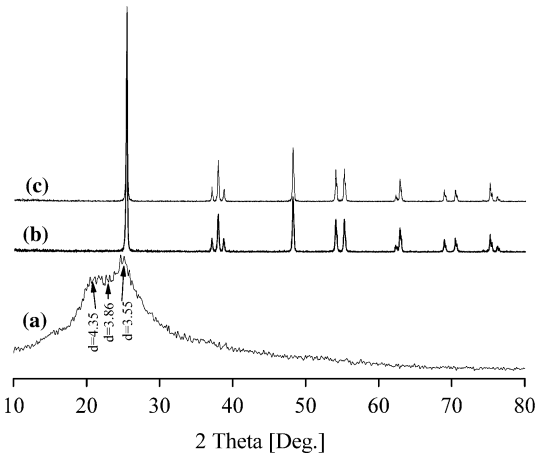

Fig. 2 The X-ray diffraction patterns of PAn doped with HCl (**a**), TiO_2 nanoparticles (**b**) and PAn/TiO_2 nanocomposites (**c**)

The X-ray diffraction patterns of PAn doped with HCl, TiO_2 nanoparticles and PAn/TiO_2 nanocomposites are showed in Fig. 2, respectively. It can be seen from Fig. 2b that the titania powder is anatase crystal, and the positions of all peaks are in good agreement with the results reported by Tang et al. [24]. In the pattern of PAn (Fig. 2a), only three broad peaks can be observed in the region of 2θ = 5.0°–30.0°, where a maximum peak is around 25.0° (d = 3.55 Å). The peak may be assigned to the scattering from PAn chains at interplanar spacing [25] and indicate that the pure PAn had also some degree of crystallinity. In the pattern of PAn/TiO_2 nanocomposites (Fig. 2c), the characteristic peaks of PAn disappear. The result suggests that the presence of TiO_2 hamper the crystalline behavior of PAn molecular chain. This is because, when the deposited PAn is absorbed on the surface of the TiO_2 nanoparticles [26], due to the restrictive effect of the surface of TiO_2 nanoparticles and the interaction of PAn and TiO_2 nanoparticles, the molecular chain of absorbed polyaniline is tethered, and the degree of crystallinity decreases. Comparing the Fig 2b and c, it can be found that the diffraction pattern of the nanocomposites is the same as TiO_2 nanoparticles. This result means that PAn deposited on the surface of TiO_2 nanoparticles has no influence on crystallization performance, of TiO_2 nanoparticles.

Chemical structure, light absorption, and ESR properties

Figure 3 shows the FTIR spectra of doped polyaniline and PAn/TiO_2 nanocomposites. The main characteristic peaks of polyaniline at 1,573 cm^{-1} (C=C stretching mode for the quinonoid unit), 1,490 cm^{-1} (C=C stretching mode for benzenoid unit), 1,302 and 1,250 cm^{-1} (C–N stretching mode of benzenoid unit), 1,144 cm^{-1} (N=Q=N, where Q represents the quinonoid unit) appear in the FTIR spectrum of the PAn/TiO_2 nanocomposites (Fig. 3b), showing the formation of PAn in the composites. Also, Fig. 3b reveals that the maximum peak of TiO_2 (625 cm^{-1}) occurred in nanocomposites. Comparing to the corresponding peaks of pure PAn (Fig. 3a) at 1,562, 1,479, 1,301, 1,246 and 1,139 cm^{-1}, the peaks of the nanocomposites shift to higher wavenumbers and the quinonoid to benzenoid band intensity ratio has also changed. These results suggest that there is a strong interaction between PAn and nanocrystalline TiO_2 [27]. When oxidant is added to the reaction system, the polymerization starts initially on the surface of TiO_2 nanoparticles, with the reaction proceeding, the PAn deposit and form a shell on the surface of TiO_2 nanoparticles. It leads to an adhesion of the PAn to TiO_2 nanoparticles [26, 28]. Because titanium is a transition metal and titanic has intense tendency to form the coordination compound with nitrogen atom in PAn molecular, such adhesion will not only constrain the motion of PAn chains, but also restricts the vibration mode in PAn molecular [29].

The UV–vis-diffuse reflectance spectra of the TiO_2 nanoparticles, PAn, and PAn/TiO_2 nanocomposites are illustrated in Fig. 4. Clearly, the prepared polyaniline/TiO_2 nanocomposites can not only strongly absorb the UV light but can also absorb the visible and near-IR light (Fig. 4c), whereas the TiO_2 can absorb light with wavelengths below 400 nm only (Fig. 4a). In the spectrum of Fig. 4b, PAn exhibits two major absorptions around 385 nm, which is related to the π–π^* transition on the PAn chains, and the absorption at 638 nm, which is contributed to polaron after doping and corresponds to localization of electron [30]. But in PAn/TiO_2 composites, the peak at 385 nm red-shifts to 427 nm and the peak at 638 nm disappears, displaced by a broad and strong absorption band with a long tail characterization (called "free-carrier-tail" by Alan et al. [31]) in the near IR region. This tail is indicative of charge carriers

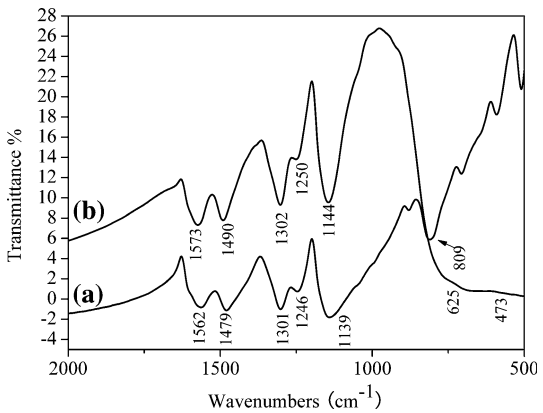

Fig. 3 The FTIR spectra of PAn doped with HCl (**a**) and PAn/TiO_2 nanocomposites (**b**)

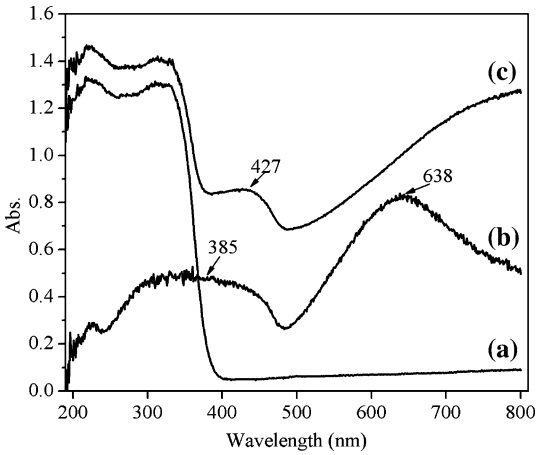

Fig. 4 The UV–vis spectra of the TiO_2 nanoparticles (**a**), PAn (**b**), and PAn/TiO_2 nanocomposites (**c**)

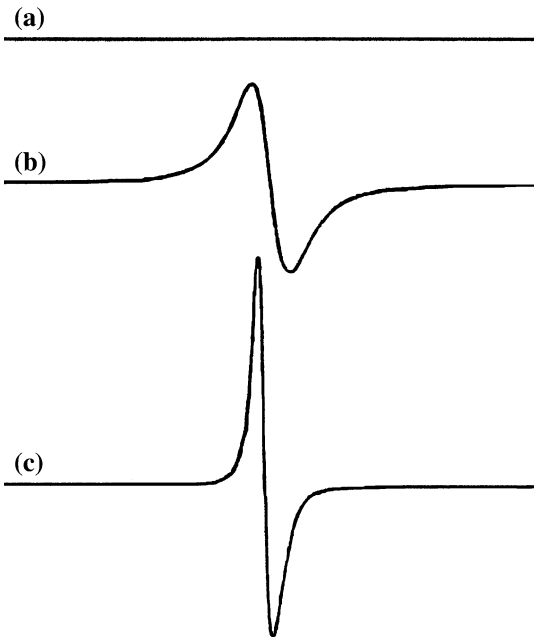

Fig. 5 The ESR spectra of TiO_2 (**a**), PAn (**b**) and PAn/TiO_2 nanocomposites (**c**)

delocalization in the polaron band favored by an extended chain conformation of the polyaniline [30]. This result reveals that in composites, the PAn is a more expanded coil molecular conformation [32], and there is an interaction between PAn molecular chains and TiO_2 nanoparticles [26]. In pure PAn, the strong interaction of chains caused π-conjugated defects, and always leads to "compact coil" conformation. While in PAn/TiO_2 composites, the TiO_2 not only eliminate the interaction of different PAn chains, but also limit the contraction of the chains. Therefore, the interaction between the adjacent isolated polarons become stronger, and the polaron band become more dispersed in energy. As a result the "free-carrier tail" appears and the localized polaron band disappears. Also, the observed enhancement of the PAn photoresponse in composites can be attributed to the increased efficiency of charge photogeneration due to a photoinduced charge transfer from the photo-induced PAn to the TiO_2 [20, 21]. The result indicate that polyaniline is capable of sensitizing TiO_2 efficiently and resulting nanocomposite photocatalyst can be activated by absorbing both the ultraviolet and visible light (λ = 190–800 nm) to give a maximum visible light harvesting, and is a promising photoelectric conversion and photocatalytic material for the efficient use of light, especially sunlight.

The ESR spectra of TiO_2, PAn and the PAn/TiO_2 nanocomposite photocatalyst are shown in Fig. 5. In the ESR experiments, no response is observed that can be attributed to electrons in TiO_2 (Fig. 5a), but the PAn shows a distinct, almost isotropic ESR signal with a g value of 2.0170 and a peak-to-peak line width ΔH_{pp} of 0.70 G (Fig. 5b). This ESR signal may be readily attributed to PAn cation radicals (polarons) [18, 33]. After being coated with PAn, a larger ESR signal is found for the sample of PAn/TiO_2 nanocomposites (Fig. 5c) with a g value of 2.0170, which is same as that of PAn. However, the ΔH_{pp} decreases to 0.22 G compared with pure PAn, indicating that the polarons in the PAn/TiO_2 are more delocalized than those in the pure PAn [34]. This response-enhancing and the line width-decreasing phenomenon will probably be due to the charge transfer from the photoexcited PAn to TiO_2 and the interaction of TiO_2 and PAn [18, 19].

Photocatalytic activities of PAn/TiO_2 nanocomposites under natural light

Under natural light irradiation and in the presence of O_2 only from air, the photocatalytic decolorization of MB in the presence or the absence of the catalysts was studied and the results are presented in Fig. 6. It is obvious that without the addition of a catalyst, the decolorization efficiency of MB is less than 3% after 90 min of irradiation (Fig. 6c), the photolysis of the MB is negligible. However, for the PAn/TiO_2 composite photocatalyst (Fig. 6b), a decolorization efficiency of 80% can be obtained after 90 min of irradiation, which is higher than that of 34% for TiO_2 nanoparticles (Fig. 6a). The photocatalytic activity of PAn/TiO_2 is remarkably superior to that of TiO_2. This result should be attributed to the efficient separation of electron and hole pairs at the interface of PAn and TiO_2 in the excited state. When PAn/TiO_2 nanocomposites are illuminated under natural light, both TiO_2 and PAn absorb the photons at their interface, then charge separation occurs at the interface. Since the conduction band of TiO_2 and the

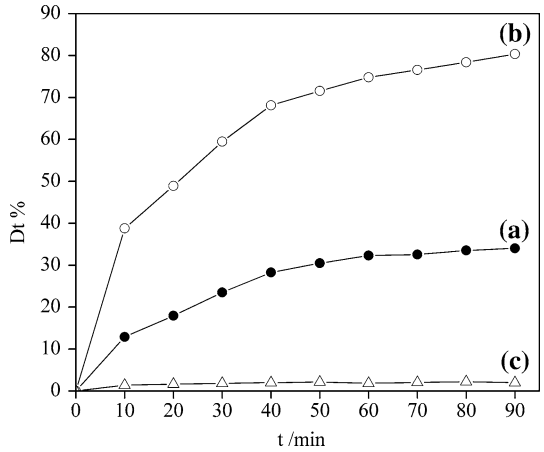

Fig. 6 Methylene blue descoloring percent with time: (**a**) TiO_2 nanoparticles; (**b**) PAn/TiO_2 nanocomposites and (**c**) methylene blue under sunlight without catalyst

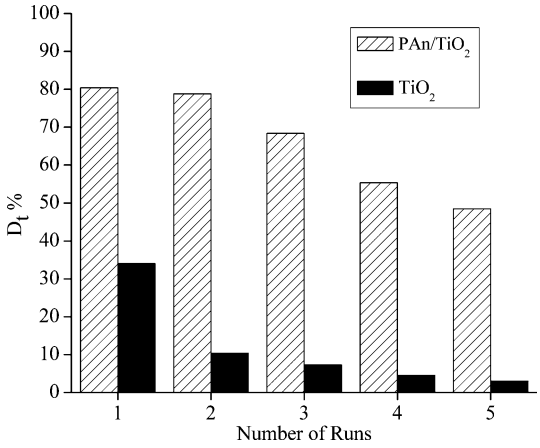

Fig. 7 Effect of number of runs on methylene blue degradation over pure TiO_2 nanoparticles and PAn/TiO_2 nanocomposites

lowest unoccupied molecular orbital (LUMO) lever of PAn are well matched for the charge transfer [21, 22]; the generated electrons by inducing PAn upon natural light irradiation can be transferred to the conduction band of TiO_2, whereas electrons in the valence band of TiO_2 are transferred into the PAn and left an electron or vacancy, enhancing the charge separation in turn promoting the photocatalytic activity of photocatalyst.

Under the same conditions, adsorption of PAn/TiO_2 to MB in the dark condition was tested. The results show that most of the adsorption occurred within 20 min, and the decolorization efficiency of MB is only about 10% at 60 min and does not change with the further increase of the time. By comparison of the values of MB removed with and without natural light, it can be affirmed that the disappearance of MB molecules is due to photocatalytic degradation instead of only to adsorption on PAn/TiO_2. Further, the IR spectra of PAn/TiO_2, before and after being used are examined (not shown here). The two IR spectra coincide with each other and no other new peaks corresponded to adsorbed MB molecules and any degraded ones are observed. This result also confirms that the decolorization of MB is related to the degradation on the PAn/TiO_2 rather than the adsorption and the PAn/TiO_2 did play a role of an efficient catalyst.

To evaluate the reusable property of catalysts, PAn/TiO_2 and TiO_2 were used for several photocatalytic runs, and each run lasted 90 min. After the first run, the catalyst was separated and used immediately for further runs without any treatment. The results in Fig. 7 show that the activity of TiO_2 decreases greatly and significant deactivation occur; only about 5% of MB can be removed within 90 min after four runs. On the other hand, the activity of PAn/TiO_2 only gradually decreases and 55% MB decolorization is still achieved after four runs. These results indicate that the PAn/TiO_2 nanocomposites are reusable and maintain relatively high activity.

Moreover, the PAn/TiO_2 nanocomposite photocatalyst had an advantage over the pure TiO_2. They had good sedimentation ability and could decant in a few minutes. Separation tests showed that the PAn/TiO_2 composite nanoparticles could easily be separated by gravity sedimentation. All catalysts could decant on the bottom of a graduate cylinder within 5 min, whereas pure TiO_2 did not decant after 2 h. Therefore, considering the separation and deactivation problem of nanosized TiO_2, the easy separation and reusable ability of PAn/TiO_2 implies that it is potentially employable in practical applications under mild condition such as natural light and oxygen from air.

Conclusion

Polyaniline (PAn) sensitized nanocrystalline TiO_2 composite photocatalyst (PAn/TiO_2) has been successfully prepared by the in situ chemical oxidation of aniline in the presence of TiO_2 nanoparticles. The presence of TiO_2 hampers the crystalline behavior of PAn and reduces its crystallinity. The results of FTIR, UV–vis and ESR confirm that there is a strong interaction between PAn and TiO_2 nanoparticles, and PAn is able to sensitize TiO_2 efficiently and the composites photocatalyst can be activated by absorbing both the ultraviolet and visible light and this would favor the photocatalytic activity of TiO_2 under natural light. As expected, the PAn/TiO_2 exhibit better photocatalytic activity in the photocatalytic degradation of MB under natural light, compared with TiO_2. This can be attributed to the charge transfer from photoexcited sensitizer to TiO_2 and efficient separation of e^--h^+ pairs. It brings about important breakthrough of photocatalytic property of TiO_2. Moreover, the composite photocatalyst

can be reused for several runs and has good sedimentation ability. Thus, the PAn/TiO_2 nanocomposites are an efficient material for decontaminating colored wastewater for reuse in textile industries under mild conditions.

Acknowledgements Authors are grateful to Prof. H. G. An, D. Q. Wu, Y. S. Wang for their constant encouragement and stimulating discussion. Y. Q. Han is thanked for his kindly supply the chemical regents. We also thank the financially support from Department of Chemistry and Key laboratory of Resources and Environmental Chemistry of West China, Hexi University.

References

1. Fujishima A, Rao TN, Tryk DA (2000) J Photochem Photobiol C: Rev 1:1
2. Konstantinou IK, Albanis TA (2004) Appl Catal B: Environ 49:1
3. Balasubramanian G, Dionysiou DD, Suidan MT, Baudin I, Laîné J-M (2004) Appl Catal B: Environ 47:73
4. Antoniou MG, Dionysiou DD (2007) Catal Today 124:215
5. Hoffmann MR, Martin ST, Choi W, Bahnemann D (1995) Chem Rev 95:69
6. Regan BÒ, Grätzel MA (1991) Nature 353:734
7. Pereraa VPS, Pitigala PKDDP, Senevirathne MKI, Tennakone K (2005) Solar Energy Mater Solar Cells 85:91
8. Iwasaki M, Hara M, Kawada H, Tada H, Ito S (2000) J Colloid Interf Sci 224:202
9. Subramanian V, Wolf E, Kamat PV (2001) J Phys Chem B 105:11439
10. Asahi R, Morikawa T, Ohwaki T, Aoki K, Taga Y (2001) Science 293:269
11. Pron A, Rannou P (2002) Prog Polym Sci 27:135
12. Shaheen SE, Brabec CJ, Padinger F, Fromherz T, Hummelen JC, Sariciftci NS (2001) Appl Phys Lett 78:841
13. Suh DJ, Park OO, Ahn T, Shim H (2002) Opt Mater 21:365
14. Ravirajan P, Haque SA, Poplavskyy D, Durrant JR, Bradley DDC, Nelson J (2004) Thin Solid Films 451–452:624
15. Kwon J, Kim P, Keum J, Kim JS (2004) Solar Energy Mater Solar Cells 83:311
16. Hebestreit N, Hofmann J, Rammelt U, Plieth W (2003) Electrochim Acta 48:1779
17. Andersona NA, Haoa E, Ai X, Hastings G, Lian TQ (2002) Phys E 14:215
18. van Hal PA, Christiaans MPT, Wienk MM, Kroon JM, Janssen RAJ (1999) J Phys Chem B 103:4352
19. Christiaans MPT, Wienk MM, van Hal PA, Kroon JM, Janssen RAJ (1999) Synth Met 101:265
20. Luzzati S, Basso M, Catellani M, Brabec CJ, Gebeyehu D, Sariciftci NS (2002) Thin Solid Films 403–404:52
21. Senadeera GKR, Kitamura T, Wada Y, Yanagida S (2004) J Photochem Photobiol A: Chem 164:61
22. Yanagida S, Senadeera GKR, Nakamura K, Kitamura T, Wada Y (2004) J Photochem Photobiol A: Chem 166:75
23. Savenije TJ, Vermeulen WMJ, de Haas MP, Warman JM (2000) Solar Energy Mater Solar Cells 61:9
24. Tang H, Prasad K, Sanjines R, Schmid PE, Levy F (1994) J Appl Phys 75:2042
25. Feng W, Sun E, Fujii A, Wu H, Nihara K, Yoshino K (2000) Bull Chem Soc Jpn 73:2627
26. Xia HS, Wang Q (2002) Chem Mater 14:2158
27. Zhang LJ, Wan MX (2003) J Phys Chem B 107:6748
28. Li XW, Wang GC, Li XX, Lu DM (2004) Appl Surf Sci 229:395
29. Somani PR, Marimuthu R, Mulik UP, Sainkar SR, Amalnerkar DP (1999) Synth Met 106:45
30. Su SJ, Kuramoto N (2000) Synth Met 114:147
31. Alan GM, Arthur JE (1995) Synth Met 69:85
32. Wu Q, Xue Z, Qi Z, Wang F (2000) Polymer 41:2029
33. Chen SA, Hwang GW (1994) J Am Chem Soc 116:7939
34. Chen SA, Hwang GW (1996) Macromolecules 29:3950